Glaucoma assessment in high myopic eyes using optical coherence tomography with long axial length normative database

Yu-Fan Chang[a,b], Yu-Chieh Ko[a,c], Chih-Chien Hsu[a,b], Mei-Ju Chen[a,c], Catherine Jui-Ling Liu[a,c*]

[a]Department of Ophthalmology, Taipei Veterans General Hospital, Taipei, Taiwan, ROC; [b]Institute of Clinical Medicine, National Yang-Ming University, Taipei, Taiwan, ROC; [c]Faculty of Medicine, National Yang-Ming University School of Medicine, Taipei, Taiwan, ROC

Abstract

Background: We investigated the performance of glaucoma assessment using RS-3000 spectral domain optical coherence tomography with a long axial length (AL) normative database versus Cirrus HD-OCT in eyes with high myopia.

Methods: This is a prospective case–control study. Eyes with AL ≥26 mm were enrolled, including 40 control eyes and 41 eyes with primary open-angle glaucoma. Each participant received OCT imaging with both devices at the same visit. We calculated the area under receiver operating characteristic curve (AUROC) for circumpapillary retinal nerve fiber layer (cpRNFL) and macular ganglion cell complex (GCC) parameters, and compared the false-positive and false-negative rates between the two devices.

Results: Both devices performed comparably well in glaucoma assessment regarding cpRNFL parameters, with the best parameter being the average cpRNFL for RS-3000 (AUROC: 0.899) and the clock-hour 7 cpRNFL for Cirrus HD (AUROC: 0.912). Regarding macular GCC parameters, although the nasal-inferior outer sector of the RS-3000 (AUROC 0.873) and the inferior-temporal sector of the Cirrus HD (AUROC 0.840) performed well in glaucoma assessment, generally speaking there was a higher false-positive rate using Cirrus HD when compared with that of RS-3000.

Conclusion: For eyes with long AL, both OCT devices are comparable in the ability of discriminating glaucoma from non-glaucoma in terms of cpRNFL parameters, while the macular GCC parameters of RS-3000 were less likely to over-diagnose glaucoma in highly myopic eyes.

Keywords: Glaucoma; High myopia; Optical coherence tomography

1. INTRODUCTION

Myopia, a risk factor for the development of glaucoma,[1–3] is highly prevalent in Asia,[4–6] and the mean magnitude of myopic refraction in most Asian populations has escalated over the past few decades.[7] Axial length (AL) is the primary determinant of non-syndromic myopia.[8] However, the ability to distinguish early glaucomatous damage from a non-glaucomatous myopic change is often challenging in myopic eyes due to morphological abnormalities in ocular structures associated with AL elongation.

Many studies have demonstrated the usefulness of spectral domain optical coherence tomography (SD-OCT) in detecting glaucomatous damage. By comparing the thickness of circumpapillary retinal nerve fiber layer (cpRNFL) and the macular ganglion cell complex (GCC) parameters in each eye to that of a built-in normative database, color codes indicating normal, suspect, or outside normal limits were shown in the summary report.[9–15] However, several researchers have cautioned about the risk of misclassification if we solely rely on numerical values or color-coded flags of OCT findings in glaucoma assessment, particularly when dealing with highly myopic eyes.[16–18] The high false-positive rate observed with SD-OCT assessments in myopia is probably due to the facts that high myopic eyes have variable disc morphologies,[19–22] smaller disc sizes,[23] thinner retinal nerve fiber layers (RNFLs),[24–26] and more temporally shifted retinal nerve fiber bundle distributions,[27] compared with normal eyes without myopia.

The RS-3000 (Nidek, Gamagori, Aichi, Japan) is an SD-OCT device equipped with built-in software that adjusts for AL-associated ocular magnifications. In addition to the typical normative database for eyes with ALs <26 mm, this model is equipped with an optional database for eyes with ALs ≥26 mm. The present study aimed to investigate whether the RS-3000 SD-OCT with the built-in software and long AL normative database (LAND) increases the accuracy in glaucoma assessment for highly myopic eyes eyes when compared with another SD-OCT device not considering these AL-associated factors (Cirrus HD-OCT, software version 6.0; Carl Zeiss Meditec Inc, Dublin, CA).

2. METHODS

This prospective, comparative, cross-sectional study was approved by the Institutional Review Broad and the Ethics

*Address correspondence. Dr. Catherine Jui-Ling Liu, Department of Ophthalmology, Taipei Veterans General Hospital, 201, Section 2, Shi-Pai Road., Taipei 112, Taiwan, ROC. E-mail address:jlliu@vghtpe.gov.tw (C.J.-L. Liu).

Conflicts of Interest Statement: The authors declare that they have no conflicts of interest related to the subject matter or materials discussed in this article.

Journal of Chinese Medical Association. (2020) 83: 313-317.

Received March 23, 2018; accepted July 9, 2019.

doi: 10.1097/JCMA.0000000000000254.

Committee of Taipei Veterans General Hospital, Taiwan. We enrolled patients with high myopia, 20–59 years of age, with or without glaucoma. This age-range matched that of subjects who contributed to the normative database of the RS-3000. Written informed consent was obtained from participants before enrollment.

All subjects received comprehensive ocular examinations, including auto-refraction, intraocular pressure (IOP), central corneal thickness, AL measured with an IOLMaster (V.5.02, Carl Zeiss Meditec, Oberkochen, Germany), slitlamp biomicroscopy, gonioscopy, fundoscopy with a hand-held lens, and fundus photography in various modes (color, red-free, and cobalt light). The SD-OCT evaluation was performed with a dilated pupil. A visual field (VF) test was performed with Humphrey automated perimetry with the Swedish Interactive thresholding algorithm (SITA) standard (i750, Carl Zeiss Meditec, Oberkochen, Germany).

All enrollees had a best-corrected visual acuity of 20/30 or better, IOP < 21 mmHg, AL ≥ 26 mm, spherical equivalent ≤ –5 D, astigmatism ≤ 3 D, and reliable SITA-Standard 24-2 VF test results within 4 months of the OCT imaging acquisition. A VF test with fixation loss ≤ 20%, false positives ≤ 15%, and false negatives ≤ 15% was regarded as reliable. Eyes were excluded when they had coexisting ocular disease (other than a refractive error or cataract); ocular inflammation; high myopia-related retinal degeneration; other neurological diseases which may cause VF defect; history of ocular surgery within 3 months; or a history of refractive surgery or ocular trauma.

2.1. Patients with primary open-angle glaucoma and myopia

Glaucoma was diagnosed based on characteristic changes in optic nerve head (ONH)/RNFL and corresponding VF loss. The ONH changes included neuroretinal rim thinning, notching, or excavation. A glaucomatous RNFL defect on fundus photography was slit-, wedge-, or band-shaped, matching RNFL distribution pattern and were wider than adjacent vessels. Glaucomatous VF defect was defined as follows; (1) conformed to patterns of retinal nerve fiber distribution; (2) had ≥3 non-edge continuous points in the same with a pattern standard deviation value <0.05 and one <0.01; and (3) with a glaucoma hemifield test classified as outside normal limits. When both eyes of one subject fulfilled all the criteria, we chose the eye with better VF for statistical analysis.

2.2. Myopic subjects without primary open-angle glaucoma

These participants served as the control group. All had normal IOPs (<21 mmHg), and unremarkable anterior segment and fundus findings, except for a tilted disc and peripapillary chorioreinal atrophy which did not interfere with cpRNFL evaluations with the SD-OCT. Subjects with general reductions in VF sensitivity or enlarged blind spots which corresponded to high myopic fundus changes were not excluded. When both eyes met the enrollment criteria, we chose the right eye for statistical analysis.

2.3. RS-3000 SD-OCT and Cirrus HD-OCT measurements

OCTs were performed with both the RS-3000 and the Cirrus HD in all participants in random order on the same day. These two devices differ in image acquisition time, retinal segmentation, and axial resolution, but their circular scan diameters for cpRNFL measurements are almost the same and their scanning center in GCC measurement is placed symmetrically on the fovea. In the RS-3000, the macular GCC was measured as the thickness from the internal limiting membrane to the inner plexiform layer; while in the Cirrus HD, it was measured from the retinal ganglion cells to the inner plexiform layer. Additionally, these two devices had different GCC map areas and partitions (Fig. 1). Images were excluded when they had signal strengths <7, poor imaging quality, vitreous opacity that affected image acquisition, marked chorioretinal degeneration, or displayed a mirroring effect, due to an extremely long AL.

2.4. Classification of abnormality

In the cpRNFL thickness analysis, the thickness was classified as abnormal when at least one of the clock-hour sectors on the map was color-coded either red (<1% of probability to be within normal range of an age-matched normal population) or yellow (<5%).[18,28,29] Similarly, the GCC was classified as abnormal when at least one of the sectors of the significance map was color-coded red or yellow. The false-positive rate of the control group and the false-negative rate of the primary open-angle glaucoma (POAG) group were calculated and compared between the two OCT devices.

2.5. Statistical analysis

All analyses were performed with SPSS software, V20.0 (Chicago, IL). Descriptive data, cpRNFL parameters, and GCC parameters were compared between the POAG and control groups with the Mann-Whitney *U* test. The areas under the receiver operating characteristic curves (AUROCs) for individual cpRNFL and GCC parameters were compared between the two devices. We used two sample test of proportion to compare the false-positive rate and false-negative rate between these two devices.

3. RESULTS

In total, 41 high myopic eyes with POAG, and 40 high myopic eyes without glaucoma (controls) were included in the final analyses. Demographic and clinical characteristics of these participants are shown in Table 1. The thickness of various cpRNFL and GCC parameters significantly differed between the control and POAG eyes, except for cpRNFL at clock-hours 3 and 4 of the RS-3000 and cpRNFL at clock-hours 12, 1, 3, 4, and 5 of the Cirrus HD-OCT.

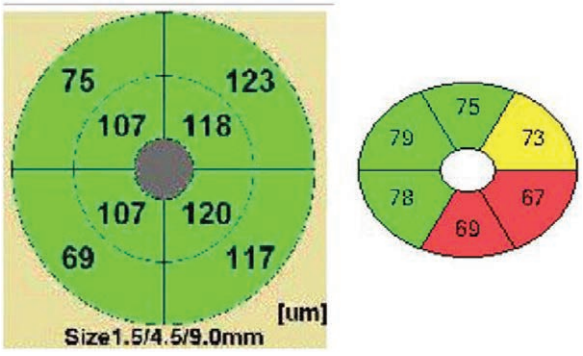

Fig. 1 Macular scanning areas, with grids denoting sectors of significance, in RS-3000 OCT and Cirrus HD-OCT. (*Left*) RS-3000 OCT uses an eight-sectored circular map (G-chart), which comprises a 9 × 9 mm² area, centered at the fovea (gray area, 1.5 mm diameter). There are four inner (4.5 mm diameter) and four outer (9 mm diameter) sectors. (*Right*) Cirrus HD-OCT uses a six-sectored elliptical map of GCIPL, which comprises a 4 × 4.8 mm² area, centered at the fovea. Number shown in each sectors represent GCC thicknesses in RS-3000, and GCIPL thicknesses in Cirrus HD. For both devices, the significance maps use three-level color coding to indicate whether the thickness of a given sector is within the normal range (green, 5 to 95% probability), borderline (yellow, 1 to 5% probability), or outside the normal range (red, < 1% probability) compared with the corresponding sector in the normative database. GCC = ganglion cell complex.

Table 1

Basic Clinical characteristics of the control and POAG groups

	Control (n = 40)	POAG (n = 41)	*p*
Age, y	39.9 ± 11.2	43.9 ± 9.5	0.086
BCVA	0.96 ± 0.14	0.92 ± 0.12	0.241
Spherical equivalent (D)	−8.21 ± 4.70	−8.94 ± 3.03	0.414
Myopic refraction (D)	−8.46 ± 3.12	−8.44 ± 2.98	0.958
Axial length	27.40 ± 1.29	27.51 ± 1.36	0.708
Central corneal thickness (μm)	565.9 ± 33.9	560.9 ± 35.1	0.514
Intraocular pressure (mmHg)	17.2 ± 2.6	15.0 ± 2.5	<0.001
Vertical C/D ratio	0.63 ± 0.18	0.81 ± 0.12	<0.001
Visual field mean deviation (dB)	−1.17 ± 1.46	−5.09 ± 3.96	<0.001
Visual field pattern standard deviation	2.06 ± 0.91	5.98 ± 3.68	<0.001
Visual field index (%)	98.3 ± 2.0	88.1 ± 10.6	<0.001

POAG = primary open-angle glaucoma; BCVA = best-corrected visual acuity; D = diopter; C/D ratio = cup-to-disc ratio.

The AUROC of each cpRNFL parameter was compared between RS-3000 and Cirrus HD-OCT. The best cpRNFL parameter for glaucoma assessment was the average RNFL (AUROC = 0.899, 95% CI, 0.824–0.973) of the RS-3000, and the RNFL at clock-hour 7 (AUROC = 0.912, 95% CI, 0.850–0.973) of the Cirrus HD, respectively. Regarding the GCC parameters, the best one to discriminate glaucoma form non-glaucoma was the nasal-inferior outer sector (AUROC = 0.873) of the RS-3000, and the inferior-temporal sector (AUROC = 0.840) of the Cirrus HD-OCT (Table 2).

Table 3 shows that in the control group, the false-positive rates tended to be lower in RS-3000 than in Cirrus HD-OCT, particularly for the GCC parameters. Overall speaking, both devices showed high sensitivity in the detection of glaucoma in eyes with high myopia, but Cirrus HD-OCT shower a lower specificity than RS-3000 (Table 4).

4. DISCUSSION

To the best of our knowledge, this was the first study to compare the RS-3000 and Cirrus HD in terms of the ability to diagnose glaucoma in highly myopic eyes with ALs ≥26 mm. We found that RS-3000 OCT with a LAND had good ability to diagnose glaucoma in these eyes with either the cpRNFL or GCC

Table 2

Area under the receiver operating characteristic curve for each cpRNFL and ganglion cell complex parameter, compared between RS-3000 SD-OCT and the Cirrus HD-OCT

AUROC parameter	RS-3000	95% CI	Cirrus	95% CI	*p*
Main RNFL thickness	0.899	0.824–0.973	0.897	0.829–0.964	0.515
Average RNFL	0.814	0.718–0.910	0.734	0.622–0.847	0.856
Superior RNFL	0.673	0.554–0.792	0.652	0.530–0.774	0.595
Nasal RNFL	0.851	0.764–0.938	0.884	0.807–0.962	0.287
Inferior RNFL	0.801	0.706–0.896	0.826	0.735–0.917	0.353
Temporal RNFL					
Clock-hour 12	0.657	0.539–0.775	0.554	0.426–0.682	0.878
Clock-hour 1	0.686	0.571–0.801	0.571	0.446–0.696	0.907
Clock-hour 2	0.725	0.610–0.840	0.714	0.599–0.829	0.552
Clock-hour 3	0.605	0.481–0.730	0.586	0.457–0.714	0.582
Clock-hour 4	0.601	0.478–0.724	0.580	0.455–0.706	0.592
Clock-hour 5	0.670	0.550–0.791	0.583	0.457–0.708	0.837
Clock-hour 6	0.770	0.666–0.874	0.791	0.691–0.892	0.388
Clock-hour 7	0.856	0.768–0.945	0.912	0.850–0.973	0.153
Clock-hour 8	0.785	0.686–0.885	0.858	0.776–0.940	0.135
Clock-hour 9	0.666	0.548–0.784	0.740	0.692–0.851	0.186
Clock-hour 10	0.784	0.684–0.884	0.815	0.722–0.908	0.327
Clock-hour 11	0.805	0.701–0.909	0.816	0.717–0.914	0.440
G-chart (RS-3000) Nasal					
Superior-inner	0.793	0.691–0.894	NA	NA	NA
Superior-outer	0.869	0.793–0.945	NA	NA	NA
Inferior-inner	0.826	0.731–0.921	NA	NA	NA
Inferior-outer	0.873	0.795–0.951	NA	NA	NA
Temporal					
Superior-inner	0.778	0.676–0.881	NA	NA	NA
Superior-outer	0.821	0.723–0.920	NA	NA	NA
Inferior-inner	0.846	0.753–0.938	NA	NA	NA
Inferior-outer	0.805	0.708–0.902	NA	NA	NA
GCIPL thickness (Cirrus)	NA	NA	0.791	0.692–0.889	NA
Average GCIPL	NA	NA	0.739	0.628–0.850	NA
Superior	NA	NA	0.683	0.566–0.801	NA
Superior-nasal	NA	NA	0.737	0.626–0.848	NA
Inferior-nasal	NA	NA	0.774	0.665–0.884	NA
Inferior					
Inferior-temporal	NA	NA	0.840	0.750–0.930	NA
Superior-temporal	NA	NA	0.813	0.718–0.909	NA

AUROC = areas under the receiver operating characteristic; cpRNFL = circumpapillary retinal nerve fiber layer; GCIPL = ganglion cell inner plexiform layer; NA = not applicable; RNFL = retinal nerve fiber layer; SD-OCT = spectral domain optical coherence tomography.

Table 3

False-positive rate in the control group and false-negative rate in the POAG group for measurements with RS-3000 OCT and Cirrus HD-OCT

	RS-3000	Cirrus HD	*p*
False-positive rate			
RNFL (Y+R)			
Quadrant map	14/40 (35%)	23/40 (57.5%)	0.045
Clock-hour map	26/40 (65%)	30/40 (75%)	0.332
RNFL (R)			
Quadrant map	7/40 (17.5%)	13/40(32.5%)	0.123
Clock-hour map	12/40 (30%)	13/40 (32.5%)	0.811
GCA (Y+R)	14/40 (35%)	35/40 (87.5%)	<0.0001
GCA (R)	7/40 (17.5%)	27/40 (67.5%)	<0.0001
GCA superior (Y+R)	9/40 (22.5%)	28/40 (70%)	<0.0001
GCA superior (R)	4/40 (10%)	13/40 (32.5%)	0.015
GCA inferior (Y+R)	12/40 (30%)	35/40 (87.5%)	<0.0001
GCA inferior (R)	6/40 (15%)	24/40 (60%)	<0.0001
	RS-3000	**Cirrus HD**	***p***
False-negative rate			
RNFL (Y+R)			
Quadrant map	4/41 (9.7%)	1/41 (2.4%)	0.168
Clock-hour map	1/41 (2.4%)	0/41 (0%)	0.321
RNFL (R)			
Quadrant map	6/41 (14.6%)	5/41 (12.2%)	0.751
Clock-hour map	5/41 (12.2%)	6/41 (14.6%)	0.751
GCA (Y+R)	3/41 (7.3%)	0/41 (0%)	0.079
GCA (R)	5/41 (12.2%)	3/41 (7.3%)	0.457
GCA superior (Y+R)	7/41 (17%)	3/41 (7.3%)	0.182
GCA superior (R)	11/41 (26.8%)	11/41 (26.8%)	1
GCA inferior (Y+R)	7/41 (17%)	2/41 (4.9%)	0.081
GCA inferior (R)	9/41 (21.9%)	4/41 (9.8%)	0.136

GCA = ganglion cell analysis; POAG = primary open-angle glaucoma; R = red-coded color, <1% of probability to be within normal range of an age-matched normal population; RNFL = retinal nerve fiber layer; Y=yellow-coded color, <5% of probability to be within normal range of an age-matched normal population.

algorithm. The cpRNFL parameters of Cirrus HD-OCT also performed well in discriminating glaucoma from non-glaucoma, but it's GCC parameters showed significantly higher false-positive rates than those of RS-3000.

Two previous studies using RS-3000 SD-OCT have shown the advantages of LAND over non-myopic normative database for detecting early glaucomatous change in highly myopic eyes.[30,31] However, the diagnostic performance of RS-3000 with a LAND versus other widely available brands of SD-OCT without a LAND remains unknown. Our study first demonstrated that the best cpRNFL parameter from both RS-3000 with a LAND and Cirrus HD without a LAND performed comparably well in glaucoma diagnosis for highly myopic eyes. These findings were in line with previous studies that show good ability of cpRNFL parameters of Cirrus HD-OCT in glaucoma assessment, despite that RNFL measurements were not adjusted for long ALs.[32]

Ohno-Matsui et al[33,34] employed high resolution 3D magnetic resonance imaging to analyze ocular topography of high myopic eyes. They showed that the globe protruded most along the central sagittal axis, in 78% of 86 eyes with pathological myopia. Furthermore, eyes with longer ALs had a high chance of displaying irregular curvature, with a temporally distorted shape. With Cirrus HD-OCT, no measurements were adjusted for AL. Consequently, the irregular curvature of the posterior pole within the relatively small macular scan area ($4 \times 4.8\,mm^2$ elliptical scan) may decrease the accuracy of macular GCC measurements with Cirrus HD-OCT in highly myopic eyes.

It is interesting to note that, in this study on eyes with high myopia, the cpRNFL parameters of both devices performed better, in general, than the macular GCC parameters for glaucoma diagnosis. This finding was inconsistent with two prior studies that investigated the impact of high myopia on the performance of another SD-OCT machine, the RTVue-100 (version 4.0.0.143, model RT-100, Optovue, Fremont, CA).[16,35,36] Those authors concluded that, although all parameters performed well for discriminating glaucoma from normal, the GCC parameters were better than cpRNFL parameters for glaucoma assessment in eyes with high myopia. One possible explanation of their findings was that the center of the GCC scan was shifted temporally by 0.75 mm (not centered on the fovea) in RTVue-100 to increase sampling of the temporal periphery, and the GCC measurement of the device included the thickness of the RNFL as well.

This study had several limitations. First, the sample size was small, and the setting was a single tertiary referral medical center; therefore, a selection bias may have existed. Myopic eyes in which glaucoma assessment is not challenging might not be included in this study, which might underestimate the diagnostic performance of these two OCT devices. However, this may not significantly affect the study outcome of our study that compared the diagnostic performance of different SD-OCT devices. Second, this cross-sectional study required a glaucomatous VF defect for making the diagnosis; therefore, the study results may not be generalized to patients with pre-perimetric glaucoma.

Table 4

Overall sensitivity and specificity of each parameters of RS-3000 and Cirrus HD-OCT for glaucoma detection

	RS-3000		Cirrus HD	
	Sensitivity, %	**Specificity, %**	**Sensitivity, %**	**Specificity, %**
RNFL (Y+R)				
Quadrant map	90.2 (76.9–97.3)	65.0 (48.3–79.4)	97.6 (87.1–99.9)	42.5 (27.0–59.1)
Clock-hour map	97.6 (87.1–99.9)	35.0 (20.6–51.7)	100 (91.4–100)	25.0 (12.7–41.2)
RNFL (R)				
Quadrant map	85.3 (70.8–94.4)	82.5 (67.2–92.7)	87.8 (73.8–95.9)	67.5 (50.9–81.4)
Clock-hour map	87.8 (73.8–95.9)	70.0 (53.5–83.4)	85.4 (70.8–94.4)	67.5 (50.9–81.4)
GCA (Y+R)	92.7 (80.1–98.5)	65.0 (48.3–79.4)	100 (91.4–100)	12.5 (4.19–26.8)
GCA (R)	87.8 (73.8–95.9)	82.5 (67.2–92.7)	92.7 (80.1–98.5)	32.5 (18.6–49.1)
GCA superior (Y+R)	82.9 (67.9–92.9)	77.5 (61.6–89.2)	92.7 (80.2–98.5)	30.0 (16.6–46.5)
GCA superior (R)	73.2 (57.1–85.8)	90.0 (76.3–97.2)	73.2 (57.1–85.8)	67.5 (50.9–81.4)
GCA inferior (Y+R)	70.7 (54.5–83.9)	70.0 (53.5–83.4)	95.1 (83.5–99.4)	12.5 (4.2–26.8)
GCA inferior (R)	78.1 (62.4–89.4)	85.0 (70.2–94.3)	90.2 (76.9–97.3)	40.0 (24.9–56.7)

GCA = ganglion cell analysis; R = red-coded color, <1% of probability to be within normal range of an age-matched normal population; RNFL = retinal nerve fiber layer; Y = yellow-coded color, <5% of probability to be within normal range of an age-matched normal population.

Third, we tried to include eyes with as long AL as possible, but it turned out to be very difficult to obtain qualified OCT images from eyes with ALs >29 mm. Since RS-3000 is not widely available globally, our study provides useful information which aids clinical judgment while using Cirrus HD-OCT as a supplement in glaucoma assessment for highly myopic eyes.

In conclusion, the cpRNFL algorithms for both RS-3000 and Cirrus HD-OCT performed equally well for discriminating between glaucoma and non-glaucoma in highly myopic eyes, but the RS-3000 outperformed the Cirrus HD in terms of macular GCC parameters. The built-in software and database of RS-3000 SD-OCT which takes AL into consideration could reduce the rate of over-diagnosis of glaucoma in highly myopic eyes.

ACKNOWLEDGMENTS

The authors declare that no funding or financial support was received in relation to this study. We would like to express our appreciation to IKI Medical Company for providing the Nidek RS-3000 SD-OCT during the study period.

REFERENCES

1. Marcus MW, de Vries MM, Junoy Montolio FG, Jansonius NM. Myopia as a risk factor for open-angle glaucoma: a systematic review and meta-analysis. *Ophthalmology* 2011;**118**:1989–94.e2.
2. Wong TY, Foster PJ, Hee J, Ng TP, Tielsch JM, Chew SJ, et al. Prevalence and risk factors for refractive errors in adult Chinese in Singapore. *Invest Ophthalmol Vis Sci* 2000;**41**:2486–94.
3. Chon B, Qiu M, Lin SC. Myopia and glaucoma in the South Korean population. *Invest Ophthalmol Vis Sci* 2013;**54**:6570–7.
4. Lin LL, Shih YF, Tsai CB, Chen CJ, Lee LA, Hung PT, et al. Epidemiologic study of ocular refraction among schoolchildren in Taiwan in 1995. *Optom Vis Sci* 1999;**76**:275–81.
5. Ling SL, Chen AJ, Rajan U, Cheah WM. Myopia in ten year old children–a case control study. *Singapore Med J* 1987;**28**:288–92.
6. Au Eong KG, Tay TH, Lim MK. Race, culture and myopia in 110,236 young Singaporean males. *Singapore Med J* 1993;**34**:29–32.
7. Pan CW, Zheng YF, Anuar AR, Chew M, Gazzard G, Aung T, et al. Prevalence of refractive errors in a multiethnic Asian population: the Singapore epidemiology of eye disease study. *Invest Ophthalmol Vis Sci* 2013;**54**:2590–8.
8. Meng W, Butterworth J, Malecaze F, Calvas P. Axial length of myopia: a review of current research. *Ophthalmologica* 2011;**225**:127–34.
9. Garas A, Vargha P, Holló G. Diagnostic accuracy of nerve fibre layer, macular thickness and optic disc measurements made with the rtvue-100 optical coherence tomograph to detect glaucoma. *Eye (Lond)* 2011;**25**:57–65.
10. Schulze A, Lamparter J, Pfeiffer N, Berisha F, Schmidtmann I, Hoffmann EM. Diagnostic ability of retinal ganglion cell complex, retinal nerve fiber layer, and optic nerve head measurements by fourier-domain optical coherence tomography. *Graefes Arch Clin Exp Ophthalmol* 2011;**249**:1039–45.
11. Seong M, Sung KR, Choi EH, Kang SY, Cho JW, Um TW, et al. Macular and peripapillary retinal nerve fiber layer measurements by spectral domain optical coherence tomography in normal-tension glaucoma. *Invest Ophthalmol Vis Sci* 2010;**51**:1446–52.
12. Tan O, Chopra V, Lu AT, Schuman JS, Ishikawa H, Wollstein G, et al. Detection of macular ganglion cell loss in glaucoma by fourier-domain optical coherence tomography. *Ophthalmology* 2009;**116**:2305–14.e1–2.
13. Mwanza JC, Oakley JD, Budenz DL, Chang RT, Knight OJ, Feuer WJ. Macular ganglion cell-inner plexiform layer: automated detection and thickness reproducibility with spectral domain-optical coherence tomography in glaucoma. *Invest Ophthalmol Vis Sci* 2011;**52**:8323–9.
14. Mwanza JC, Durbin MK, Budenz DL, Sayyad FE, Chang RT, Neelakantan A, et al. Glaucoma diagnostic accuracy of ganglion cell-inner plexiform layer thickness: comparison with nerve fiber layer and optic nerve head. *Ophthalmology* 2012;**119**:1151–8.
15. Takayama K, Hangai M, Durbin M, Nakano N, Morooka S, Akagi T, et al. A novel method to detect local ganglion cell loss in early glaucoma using spectral-domain optical coherence tomography. *Invest Ophthalmol Vis Sci* 2012;**53**:6904–13.
16. Kim NR, Lee ES, Seong GJ, Kang SY, Kim JH, Hong S, et al. Comparing the ganglion cell complex and retinal nerve fibre layer measurements by fourier domain OCT to detect glaucoma in high myopia. *Br J Ophthalmol* 2011;**95**:1115–21.
17. Hsu SY, Chang MS, Ko ML, Harnod T. Retinal nerve fibre layer thickness and optic nerve head size measured in high myopes by optical coherence tomography. *Clin Exp Optom* 2013;**96**:373–8.
18. Kim NR, Lim H, Kim JH, Rho SS, Seong GJ, Kim CY. Factors associated with false positives in retinal nerve fiber layer color codes from spectral-domain optical coherence tomography. *Ophthalmology* 2011;**118**:1774–81.
19. Grossniklaus HE, Green WR. Pathologic findings in pathologic myopia. *Retina* 1992;**12**:127–33.
20. Chihara E, Chihara K. Covariation of optic disc measurements and ocular parameters in the healthy eye. *Graefes Arch Clin Exp Ophthalmol* 1994;**232**:265–71.
21. Jonas JB, Dichtl A. Optic disc morphology in myopic primary open-angle glaucoma. *Graefes Arch Clin Exp Ophthalmol* 1997;**235**:627–33.
22. Tay E, Seah SK, Chan SP, Lim AT, Chew SJ, Foster PJ, et al. Optic disk ovality as an index of tilt and its relationship to myopia and perimetry. *Am J Ophthalmol* 2005;**139**:247–52.
23. Savini G, Barboni P, Parisi V, Carbonelli M. The influence of axial length on retinal nerve fibre layer thickness and optic-disc size measurements by spectral-domain OCT. *Br J Ophthalmol* 2012;**96**:57–61.
24. Kimura Y, Hangai M, Morooka S, Takayama K, Nakano N, Nukada M, et al. Retinal nerve fiber layer defects in highly myopic eyes with early glaucoma. *Invest Ophthalmol Vis Sci* 2012;**53**:6472–8.
25. Leung CK, Yu M, Weinreb RN, Mak HK, Lai G, Ye C, et al. Retinal nerve fiber layer imaging with spectral-domain optical coherence tomography: interpreting the RNFL maps in healthy myopic eyes. *Invest Ophthalmol Vis Sci* 2012;**53**:7194–200.
26. Payman AK, Salih M. Evaluation of peripapillary retinal nerve fiber layer thickness in myopic eyes by spectral-domain optical coherence tomography. *J Glaucoma* 2012;**21**:41–4.
27. Kang SH, Hong SW, Im SK, Lee SH, Ahn MD. Effect of myopia on the thickness of the retinal nerve fiber layer measured by cirrus HD optical coherence tomography. *Invest Ophthalmol Vis Sci* 2010;**51**:4075–83.
28. Kim KE, Jeoung JW, Park KH, Kim DM, Kim SH. Diagnostic classification of macular ganglion cell and retinal nerve fiber layer analysis: differentiation of false-positives from glaucoma. *Ophthalmology* 2015;**122**:502–10.
29. Hwang YH, Kim YY, Kim HK, Sohn YH. Ability of cirrus high-definition spectral-domain optical coherence tomography clock-hour, deviation, and thickness maps in detecting photographic retinal nerve fiber layer abnormalities. *Ophthalmology* 2013;**120**:1380–7.
30. Nakanishi H, Akagi T, Masanori Hangai, Kimura Y, Suda K, Kumagai KK, et al. Sensitivity and specificity for detecting early glaucoma in eyes with high myopia from normative database of macular ganglion cell complex thickness obtained from normal non-myopic or highly myopic Asian eyes. *Graefes Arch Clin Exp Ophthalmol* 2015; DOI 10.1007/s00417-015-3026-y.
31. Chen HS, Liu CH, Lu DW. Comparison of glaucoma diagnostic accuracy of macular ganglion cell complex thickness based on nonhighly myopic and highly myopic normative database. *Taiwan J Ophthalmol* 2016;**6**:15–20.
32. Choi YJ, Jeoung JW, Park KH, Kim DM. Glaucoma detection ability of ganglion cell-inner plexiform layer thickness by spectral-domain optical coherence tomography in high myopia. *Invest Ophthalmol Vis Sci* 2013;**54**:2296–304.
33. Ohno-Matsui K, Akiba M, Modegi T, Tomita M, Ishibashi T, Tokoro T, et al. Association between shape of sclera and myopic retinochoroidal lesions in patients with pathologic myopia. *Invest Ophthalmol Vis Sci* 2012;**53**:6046–61.
34. Moriyama M, Ohno-Matsui K, Hayashi K, Shimada N, Yoshida T, Tokoro T, et al. Topographic analyses of shape of eyes with pathologic myopia by high-resolution three-dimensional magnetic resonance imaging. *Ophthalmology* 2011;**118**:1626–37.
35. Shoji T, Sato H, Ishida M, Takeuchi M, Chihara E. Assessment of glaucomatous changes in subjects with high myopia using spectral domain optical coherence tomography. *Invest Ophthalmol Vis Sci* 2011;**52**:1098–102.
36. Shoji T, Nagaoka Y, Sato H, Chihara E. Impact of high myopia on the performance of SD-OCT parameters to detect glaucoma. *Graefes Arch Clin Exp Ophthalmol* 2012;**250**:1843–9.